A Phase I Dose-Escalation Study of Sibrotuzumab in Patients with Advanced or Metastatic Fibroblast Activation Protein-positive Cancer[1]

Andrew M. Scott,[2] Greg Wiseman, Sydney Welt, Alex Adjei, Fook-Thean Lee, Wendie Hopkins, Chaitan R. Divgi, Lorelei H. Hanson, Paul Mitchell, Denise N. Gansen, Steven M. Larson, James N. Ingle, Eric W. Hoffman, Paul Tanswell, Gerd Ritter, Leonard S. Cohen, Peter Bette, Lisa Arvay, Andree Amelsberg, Dan Vlock, Wolfgang J. Rettig, and Lloyd J. Old

Ludwig Institute for Cancer Research, Melbourne Tumour Biology Austin, and Repatriation Medical Centre, Melbourne, 3084 Australia [A. M. S., F-T. L., W. H., P. M.]; Mayo Clinic, Rochester, Minnesota 55905 [G. W., A. Ad., L., H. H., D. N. G., J. N. I.]; Memorial Sloan Kettering Cancer Center, New York, New York 10021 [S. W., C. R. D., S. M. L.]; Ludwig Institute for Cancer Research, New York, New York 10158 [S. W., E. W. H., G. R., L. S. C., L. J. O.]; Boehringer Ingelheim Pharma KG, Biberach, 88397 Germany [P. T., P. B., W. J. R.]; and Boehringer Ingelheim Pharmaceuticals Inc., Ridgefield, Connecticut 06877-0368 [L. A., A. Am., D. V.]

ABSTRACT

Purpose: **The purpose of this research was to determine the safety, immunogenicity, pharmacokinetics, biodistribution, and tumor uptake of repeat infusions of a complementarity-determining region grafted humanized antibody (sibrotuzumab) directed against human fibroblast activation protein (FAP).**

Experimental Design: **A Phase I open-label dose escalation study was conducted in patients with cancers epidemiologically known to be FAP positive. Patients were entered into one of four dosage tiers of 5, 10, 25, or 50 mg/m^2 sibrotuzumab, administered weekly for 12 weeks, with trace labeling with 8–10 mCi of ^{131}I in weeks 1, 5, and 9.**

Results: **A total of 26 patients were entered into the trial (15 males and 11 females; mean age, 59.9 years; age range, 41–81 years). Twenty patients had colorectal carcinoma, and 6 patients had non-small cell lung cancer. A total of 218 infusions of sibrotuzumab were administered during the first 12 weeks of the study, with 24 patients being evaluable. One patient received an additional 96 infusions on continued-use phase for a total of 108 infusions over a 2-year period, and 1 patient received an additional 6 infusions on continued use. There were no objective tumor responses. Only one episode of dose-limiting toxicity was observed. Therefore, a maximum tolerated dose was not reached. Treatment-related adverse events were observed in 6 patients during the infusional monitoring period. Four of the 6 patients, 3 of whom had associated positive serum human antihuman antibody, were removed from the study because of clinical immune responses. Gamma camera images of [^{131}I]sibrotuzumab demonstrated no normal organ uptake of sibrotuzumab, with tumor uptake evident within 24–48 h after infusion. Analysis of pharmacokinetics demonstrated a similar mean terminal $t_{1/2}$ of 1.4–2.6 days at the 5, 10, and 25 mg/m^2 dose levels, and with a longer mean $t_{1/2}$ of 4.9 days at the 50 mg/m^2 dose level.**

Conclusion: **Repeat infusions of the humanized anti-FAP antibody sibrotuzumab can be administered safely to patients with advanced FAP-positive cancer.**

INTRODUCTION

The growth of solid neoplasms, including epithelial cancers (carcinomas), beyond a diameter of about 1–2 mm requires the formation of a supporting tumor stroma to ensure the supply of nutrients for tumor cell survival and growth (1). In carcinomas, such as breast, colorectal, or lung cancers, the supporting tumor stroma comprises two major cell types: newly formed blood vessels and activated tumor stromal fibroblasts. The tumor stroma compartment represents a major component of the mass in most carcinomas, with 20–50% commonly seen in breast, lung, and colorectal cancers and reaching >90% in carcinomas with desmoplastic reactions. Unlike the malignant epithelial cells of carcinomas, the tumor capillary endothelial cells and activated tumor stromal fibroblasts are not transformed genetically, do not permit overgrowth of clonal variants, and do not show the genetic and phenotypic heterogeneity observed in the malignant cells. However, they differ from resting capillary endothelial cells and resting fibrocytes of normal adult tissues in morphology, molecular structure (as determined with antibody probes), gene expression profile, and production of biologically important mediators and proteases (2, 3).

The concept of targeting antigens expressed selectively on the surface of tumor capillary endothelial cells or in tumor stroma has emerged as a promising new area of cancer therapeutics. A critical element in this approach is to identify antigens highly expressed in tumors but with suitably restricted expression patterns in normal tissues (4). For targeting tumor stroma, the most advanced studies are those involving the mouse

Received 10/18/02; revised 1/8/03; accepted 1/9/03.
The costs of publication of this article were defrayed in part by the payment of page charges. This article must therefore be hereby marked *advertisement* in accordance with 18 U.S.C. Section 1734 solely to indicate this fact.
[1] Supported by Boehringer Ingelheim Pharma KG.
[2] To whom requests for reprints should be addressed, at Ludwig Institute for Cancer Research, Level 1, Harold Stokes Building, Austin and Repatriation Medical Centre, Studley Road, Heidelberg, Victoria, 3084 Australia. Phone: 613-9496-5876; Fax: 613-9496-5892; E-mail: ams@austin.unimelb.edu.au.

mAb,[3] F19, which is directed against activated tumor stromal fibroblasts (3, 5). Immunohistochemical studies with a range of normal and neoplastic human tissues have shown no F19 immunoreactivity in any normal adult organs tested, except for a subset of endocrine cells in the pancreatic islets, presumably glucagon-producing A cells (3, 5). Tests with human tumor tissues have identified two distinct patterns of F19 immunoreactivity: a proportion of soft tissue and bone sarcomas, notably malignant fibrous histiocytomas, express the F19 antigen as a classical tumor antigen on transformed cells (5), and a large proportion of carcinomas of the breast, colorectum, lung, pancreas, stomach, and esophagus, as well as squamous cell carcinomas of the head and neck (*i.e.*, >90% of cases studied) show strong and consistent F19 immunoreactivity in their tumor stromal fibroblast compartment (3). Identical patterns of F19 immunoreactivity have been detected in primary and metastatic tumors. Among the non-neoplastic lesional tissues examined by immunohistochemistry, F19 immunoreactivity has been observed in the activated fibroblast compartment of healing wounds (3), rheumatoid arthritis, and liver cirrhosis (6).

The cell surface molecule recognized by mAb F19 on activated fibroblasts and certain sarcoma cell lines has been identified (7, 8), and molecularly cloned (9) and designated FAPα (9) or FAP (10). FAP is a novel type II membrane-bound glycoprotein belonging to the serine protease gene family, and is known to have dipeptidyl peptidase activity (11, 12). Whereas expression of murine FAP in transfected cell lines has been shown to enhance tumor growth *in vivo*, the physiological role of FAP is yet to be determined, and the factors responsible for tumor induction of FAP are unknown (13). Investigation of the effects of targeting FAP in tumor with an animal model has not been possible, because there is no suitable transgenic mouse model. Nevertheless, therapeutic strategies afforded by targeting of FAP in human tumor by mAbs include mediation of immune effector function effects on stroma, and the delivery of radioisotopes, drugs, or toxins to tumor, which could result in stromal ablation and disruption of nutrient supply to tumor cells, or direct effects on tumor cells causing cell death.

Two Phase I quantitative biodistribution studies with ^{131}I-labeled mAb F19 in presurgical patients with hepatic metastasis from colorectal cancer, and in soft tissue sarcoma, have been performed previously (14, 15). These studies demonstrated the proof in principle of stromal targeting, with selective mAb F19 accumulation in tumor demonstrated by biodistribution imaging studies and biopsy analysis, and minimal localization to any normal tissue (14, 15).

On the basis of the results with the murine mAb F19, and to address problems of immune responses to murine antibodies, a humanized version of the mAb F19 (sibrotuzumab) has been developed. The humanization was performed using the complementarity determining region grafting strategy with preservation of selected framework region residues (16). The humanized antibody sibrotuzumab has been shown to bind to FAP *in vitro* in the same manner as its murine counterpart, but has not been shown to affect FAP enzymatic activity. This first-in-humans clinical trial was designed to investigate the safety of increasing doses of sibrotuzumab, and also to investigate the effect of escalating protein doses on pharmacokinetics and biodistribution of the humanized antibody, which may have significant implications in the optimal dose for targeting of tumors. We report here the results of the first human clinical study of sibrotuzumab.

MATERIALS AND METHODS

Sibrotuzumab Production. Sibrotuzumab was produced under GMP conditions by Boehringer Ingelheim Pharma KG. The trial was conducted under an Investigational New Drug application from the United States Food and Drug Administration, and was approved by the Institutional Research Ethics Committee of all of the study sites.

Trial Design. This trial was a multicenter, open-label, dose-escalation Phase I study. The objectives of this trial were to assess the safety, immunogenicity, pharmacokinetics, and biodistribution associated with increasing doses of sibrotuzumab administered weekly by i.v. infusion at doses of 5 mg/m^2, 10 mg/m^2, 25 mg/m^2, and 50 mg/m^2. Twelve infusions of sibrotuzumab were administered at weekly intervals, with infusions 1, 5, and 9 trace labeled with 8–10 mCi of ^{131}I. Blocking of thyroid uptake of free ^{131}I was performed in all of the patients with oral saturated solution potassium iodide or Lugol's solution, beginning before each [^{131}I]sibrotuzumab infusion, and continuing for 1–2 weeks. Six patients were entered at each dose level for evaluation of toxicity. Dose escalation was performed only after 3 patients had received 4 weeks of treatment, with no evidence of DLT. DLT was defined as any CTC grade 3 drug-related nonhematologic toxicity, except nausea or vomiting, and any CTC grade 4 drug related toxicity, including vomiting. All of the doses of sibrotuzumab were prepared in 100 ml of normal saline containing 5% human serum albumin. Sibrotuzumab was administered weekly by i.v. infusion over a period of 60 min.

Patients. Eligibility criteria for entry into the trial were: (*a*) patients with one of the following histologically confirmed malignancies: colorectal, non-small cell lung, breast, or head and neck cancer; (*b*) disease that was advanced, nonresectable, and/or metastatic, and had failed or refused conventional treatment; (*c*) Karnofsky performance status ≥70; (*d*) measurable or evaluable disease; (*e*) expected survival of ≥4 months; (*f*) ≥18 years of age; (*g*) absolute granulocyte count ≥1.5 × 10^9/liter; (*h*) platelet count >100 × 10^9/liter; (*i*) serum creatinine ≤2.0 mg/dl (0.20 mmol/liter); alanine aminotransferase/aspartate aminotransferase ≤3 × upper limit of normal; (*j*) bilirubin <2 mg/dl (34 μmol/liter); and (*k*) ability to provide written informed consent. Patients with active metastatic disease to the

[3] The abbreviations used are: mAb, monoclonal antibody; FAP, fibroblast activating protein; DLT, dose-limiting toxicity; SPECT; single photon emission computed tomography; HAHA, human antihuman antibody; C_{max}, maximum serum concentration; AUC, area under the serum concentration curve extrapolated to infinite time; CL, total serum clearance; V_c, volume of distribution, central compartment; V_{ss}, volume of distribution at steady state; $t_{1/2\alpha}$, half-life of the initial phase of disposition; $t_{1/2\beta}$, half-life of the terminal phase of disposition; %AUCβ proportion of area under the serum concentration curve under the terminal phase of disposition; $C_{max(ss)}$, peak plasma concentrations at steady state $C_{min(ss)}$, trough plasma concentrations at steady state; CTC, National Cancer Institute Common Toxicity Criteria.

central nervous system; exposure to an investigational agent, systemic chemotherapy, immunotherapy, or radiation therapy within 4 weeks before study entry; previous treatment with a murine, chimeric, or humanized antibody and/or antibody fragment; and any serious illness were excluded from this study. Patients who had not fully recovered from surgery as evidenced by incomplete granulation, infection, or localized edema at the incision site; who had autoimmune disease or hypertrophic skin conditions; women who were breast feeding or pregnant; and men or women of child-bearing potential who were unwilling to use a medically acceptable method of contraception were also excluded. Concurrent use of systemic corticosteroids or immunosuppressant agents was not allowed.

Radiolabelling of Sibrotuzumab. The antibody sibrotuzumab was labeled with ^{131}I by the chloramine-T method (17). The labeled mixture was purified by chromatography on columns of Sephadex G50 (Amersham Pharmacia, Uppsala, Sweden) equilibrated with 1% human serum albumin in saline. Radiochemical purity of labeled antibody was analyzed by instant-thin layer chromatography-silica gel using 10% w/v trichloroacetic acid as solvent, and >95% radiochemical purity was required before patient infusion. The immunoreactivity of antibody sibrotuzumab after radiolabeling was determined using the Lindmo assay as described previously (17) and HT 1080 clone 33 FAP-positive target cells.

Gamma Camera Imaging. Whole body images of [^{131}I]sibrotuzumab biodistribution were obtained in patients on day 0 after infusion of [^{131}I]sibrotuzumab, and on at least 4 additional occasions up to day 7 after infusion. Using a dual-headed gamma camera, anterior and posterior images were obtained simultaneously. Images were collected using high-energy, high-resolution collimation. SPECT images of a region of the body with known tumor were also obtained on at least one occasion during this period.

Biodistribution Analysis of [^{131}I]Sibrotuzumab. The biodistribution of [^{131}I]sibrotuzumab was evaluated from sequential whole body images obtained in each patient for 1 week after [^{131}I]sibrotuzumab infusions. The distribution pattern of [^{131}I]sibrotuzumab was determined both for patients within each dose level and across dose levels, and in individual patients for sequential [^{131}I]sibrotuzumab infusions. Comparison of biodistribution data to results of HAHA analysis, as well as clinical adverse events related to sibrotuzumab infusion, was also performed.

Pharmacokinetics. Multiple serum samples were collected after sibrotuzumab infusions for pharmacokinetics of ^{131}I total radioactivity by gamma counting in weeks 1, 5, and 9. Sibrotuzumab protein was measured by ELISA in these samples, and in additional peak and trough samples that were taken before and immediately after each unlabelled sibrotuzumab infusion. The ELISA was a noncompetitive assay using anti-sibrotuzumab idiotype mAbs, with a lower limit of quantitation of 10 ng/ml and an intra-assay precision of 2.5–4.6% over the measurement range. Compartmental model fitting (1 or 2 compartments) was performed on data sets of individual patients using the program TOPFIT (18). Single dose fitting was performed for the [^{131}I]sibrotuzumab data, because the interval between radioactive doses was more than five times longer than the maximum half-life of sibrotuzumab. Multiple dose fitting procedures were used for the ELISA data. The following parameters were calculated from the model: C_{max}, AUC, CL, V_c, V_{ss}, $t_{1/2\alpha}$ and $t_{1/2\beta}$, %AUCβ, $C_{max(ss)}$ and $C_{min(ss)}$.

HAHA. For HAHA measurements, serum samples were taken before each infusion and up to 4 weeks after the last infusion. HAHA analysis was performed by Biacore (19), and a sandwich type "double antigen" ELISA based on a reported format (20). Sibrotuzumab was used as capture antigen and horseradish peroxidase-labeled sibrotuzumab as a detection reagent. For Biacore measurements, a cutoff value of 26 response units was calculated from the individual response values of 25 predose samples (19). In the ELISA, a standard curve was constructed using defined amounts of a murine monoclonal anti-sibrotuzumab idiotype antibody. The lower limit of quantitation of the ELISA was 20 ng/ml anti-idiotype equivalents, and this was defined to be the cutoff value. All of the samples with a response above the cutoff value in either the Biacore assay or ELISA were considered to indicate a positive anti-sibrotuzumab immune response. A positive anti-sibrotuzumab immune response was characterized additionally in Biacore blocking experiments using mAb F19 (the parental murine mAb from which sibrotuzumab has been engineered), and human IgG1 control mAb as described (19).

RESULTS

Patient Characteristics. A total of 26 patients were entered into the trial (15 males and 11 females; mean age, 59.9 years; age range, 41–81 years). Twenty patients had colorectal carcinoma, and 6 patients had non-small cell lung carcinoma. The patient demographics, including prior treatment and sites of disease on study entry, and number of infusions of sibrotuzumab received, are detailed in Table 1. Two of the 26 patients withdrew from the study before completing 4 weeks of treatment without experiencing DLT and were replaced. A total of 218 infusions of sibrotuzumab were administered during the first 12 weeks of the study, with 24 patients being evaluable. One patient received an additional 96 infusions on continued-use phase for a total of 108 infusions over a 2-year period, and 1 patient received an additional 6 infusions on continued use.

Adverse Events. Adverse events related to sibrotuzumab are listed in Table 2. One episode of DLT was observed at the 50 mg/m^2 dose level, and, therefore, maximum tolerated dose was not reached. This particular patient experienced back pain (CTC grade 3), which resolved within 30 min, but this episode was dose limiting according to protocol definitions. The patient also experienced flushing, hypertension, fever, and rigors. Some of these symptoms, as well as coughing, dyspnea, and hypoxia (secondary to rigors) were considered related to sibrotuzumab in another 5 patients. Three of these 6 patients were removed from study because of symptoms of clinical immune response associated with positive serum HAHA.

Biodistribution Analysis of [^{131}I]Sibrotuzumab. The biodistribution pattern after infusion of [^{131}I]sibrotuzumab was consistent with blood pool activity, with no normal organ increased uptake after the first infusion of [^{131}I]sibrotuzumab in all of the patients at all of the dose levels (Figs. 1–3). Clearance from all of the normal organs was observed to occur over the 1 week of imaging consistent with blood pool clearance. In some

Table 1 Patient characteristics

Dose group (mg/m^2)	Patient ID	Gender	KPS[a]	Age (years)	BSA (m^2)	No. of infusions administered	Tumor type[b]	Prior treatment[c]	Sites of disease[d]
5	103	Female	90	81	1.5	7	NSCLC	RT and CT	Liver
5	104	Male	80	54	2.11	9	NSCLC	RT and CT	Lung
5	137	Female	90	48	1.82	12	Colorectal	CT and IT	Liver
5	138	Male	80	60	1.61	2	NSCLC	CT	Lt lung, Rt and Lt adrenal
5	139	Female	80	56	1.52	5	Colorectal	CT	Liver
5	140	Male	90	76	1.86	108	Colorectal	CT and RT	Liver
5	142	Male	90	60	2.25	12	Colorectal	CT and RT	Azygo-oesophageal LN, liver, lung, para-aortic LN
10	101	Male	100	70	2.08	9	NSCLC	RT and CT	Adrenal
10	102	Female	70	64	2.21	8	Colorectal	RT, IT and CT	Rt and Lt lung
10	108	Female	80	43	1.8	7	Colorectal	CT	Retroperitoneal and mesenteric LN
10	128	Female	90	69	1.89	4	Colorectal	CT	Liver
10	134	Male	90	45	1.86	12	Colorectal	None	Liver
10	141	Male	70	43	1.85	12	NSCLC	CT	Rt and Lt lung, mediastinal LN
25	105	Male	100	55	2.31	8	Colorectal	CT	Liver
25	106	Male	90	59	2.63	5	Colorectal	CT	Rt and Lt lung
25	125	Male	90	57	2.18	8	Colorectal	CT	Lt lung, abdominal LN
25	126	Female	90	44	1.63	10	Colorectal	RT and CT	Liver, spleen
25	143	Male	90	71	2.26	12	Colorectal	CT and surgery	Liver
25	146	Male	90	60	1.84	8	Colorectal	CT	Rt and Lt lung, liver
50	107	Female	80	65	1.92	12	Colorectal	RT and CT	Rt and Lt lung
50	127	Female	70	77	1.8	1	Colorectal	CT	Rt and Lt lung, liver, chest and abdominal LN
50	129	Male	90	77	1.8	4	Colorectal	CT	Rt lung
50	130	Female	90	41	1.6	4	Colorectal	RT and CT	Hilum, Lt lung
50	144	Female	90	56	1.76	18	NSCLC	RT and CT	Lt neck, Rt lung
50	145	Male	90	56	2.03	11	Colorectal	CT	Liver
50	147	Male	100	71	1.82	12	Colorectal	RT and CT	Rt and Lt lung, liver

[a] Abbreviations: KPS, Karnofsky Performance Status; BSA, Body Surface Area.
[b] NSCLC, non-small cell lung carcinoma.
[c] RT, radiotherapy; CT, chemotherapy; IT, immunotherapy.
[d] Lt, left; Rt, right; LN, lymph nodes.

Table 2 Adverse events related to sibrotuzumab

	Treatment at onset									
	5 mg/m^2		10 mg/m^2		25 mg/m^2		50 mg/m^2		Total	
	n	%	*n*	%	*n*	%	*n*	%	*n*	%
Summary data										
Total number of patients	7	100	6	100	6	100	7	100	26	100
Total with any adverse event related to sibrotuzumab	1	14	2	33	1	17	2	29	6	23
Adverse events										
Anorexia	—	—	—	—	—	—	1 (1)	14	1	4
Flushing	1 (1)[a]	14	1 (1)	17	1 (1)	17	1 (1)	14	4	15
Back pain	—	—	—	—	—	—	1 (3)	14	1	4
Fever	—	—	—	—	—	—	1 (2)	14	1	4
Rigors	1 (2)	14	1 (1)	17	1 (2)	17	2 (2)	29	5	19
Hypertension	—	—	1 (1)	17	—	—	1 (2)	14	2	8
Coughing	—	—	—	—	1 (2)	17	—	—	1	4
Dyspnea	—	—	—	—	1 (2)	17	—	—	1	4
Hypoxia	1 (1)	14	—	—	—	—	—	—	1	4

[a] Figure in parentheses indicates CTC grade for adverse event.

patients minor uptake of ^{131}I was evident in the thyroid, and less frequently in the stomach, consistent with free ^{131}I uptake (Fig. 3). In 3 patients minor low-grade uptake in the knees and shoulders was observed, with no clinical symptoms of arthritis (Fig. 3). There was no difference in the observed pattern of biodistribution of [^{131}I]sibrotuzumab between dose levels.

Repeat infusions of [^{131}I]sibrotuzumab, when HAHA was not present, showed a similar pattern of blood pool clearance and normal organ uptake compared with the first [^{131}I]sibrotuzumab infusion. This was observed for up to 10 infusions of [^{131}I]sibrotuzumab over four cycles in 1 patient (Fig. 3).

High, selective uptake of [^{131}I]sibrotuzumab in sites of

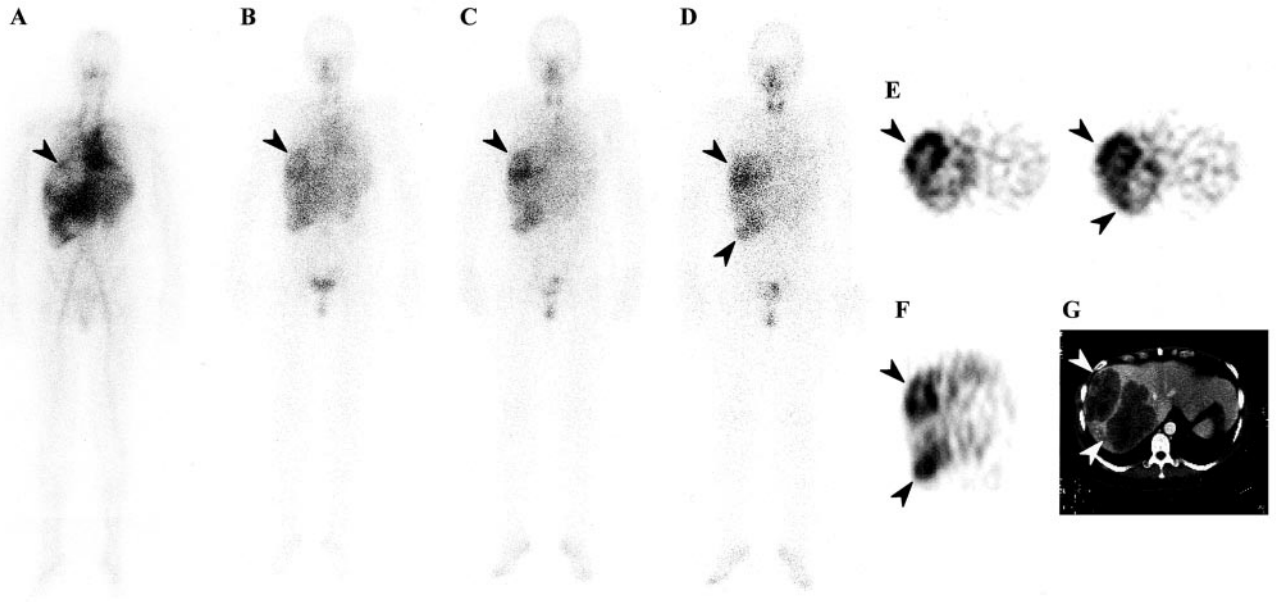

Fig. 1 Biodistribution and targeting of [^{131}I]sibrotuzumab to metastatic colorectal carcinoma in patient 137, infusion 1, 5 mg/m^2 dose level. *A*, day 0 anterior whole body gamma camera image showing blood pool activity only. Metastatic lesions in the liver show reduced blood pool activity (*arrow*). *B*, day 2; *C*, day 4; *D*, day 7 postinfusion, showing excellent uptake in metastatic lesions in the liver, and in omentum (*arrows*). *E*, transverse and (*F*) coronal SPECT images of the liver showing high specific uptake in metastatic lesions: central necrosis in liver metastases is also evident. *G*, computed tomography through same transverse plane as SPECT image in *E*.

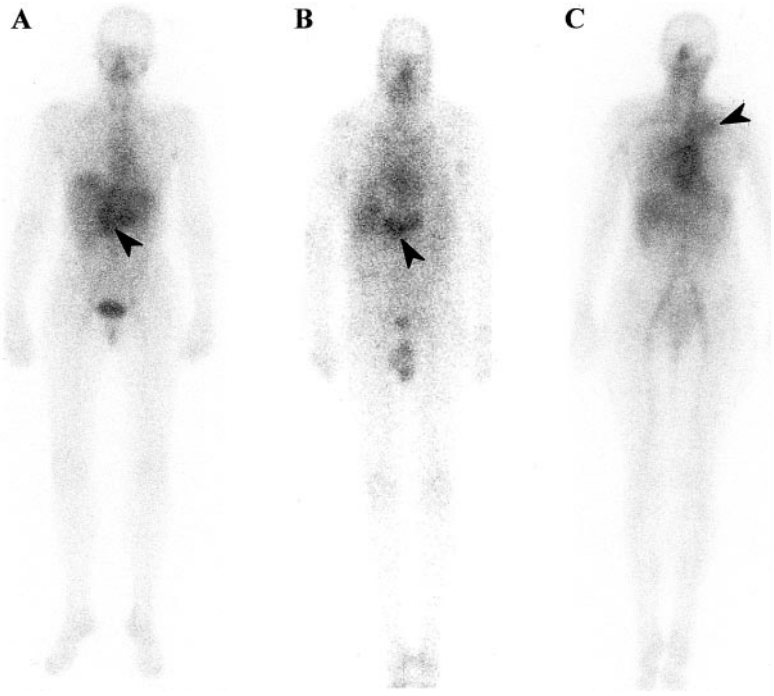

Fig. 2 Targeting of [^{131}I]sibrotuzumab to metastatic tumors (*black arrows*). Anterior whole body gamma camera images day 3 after infusion of: (*A*) patient 139, 5 mg/m^2 dose level, showing targeting to liver metastases of colorectal carcinoma; (*B*) patient 105, 25 mg/m^2 dose level, liver metastases of colorectal carcinoma; (*C*) patient 144, 50 mg/m^2 dose level, non-small cell lung carcinoma.

metastatic disease >1.5 cm was evident in all of the patients, often as early as day 2 after infusion (Figs. 1–3). The targeting of metastatic disease was observed after multiple infusions of sibrotuzumab (Fig. 3), indicating the selective and consistent targeting of sibrotuzumab to tumor.

HAHA was associated with altered biodistribution compared with the first infusion datasets in all of the patients where HAHA was present at the time of [^{131}I]sibrotuzumab infusion (Table 3). In 3 patients (patients 139, 142, and 106) altered biodistribution was associated with relative increased liver up-

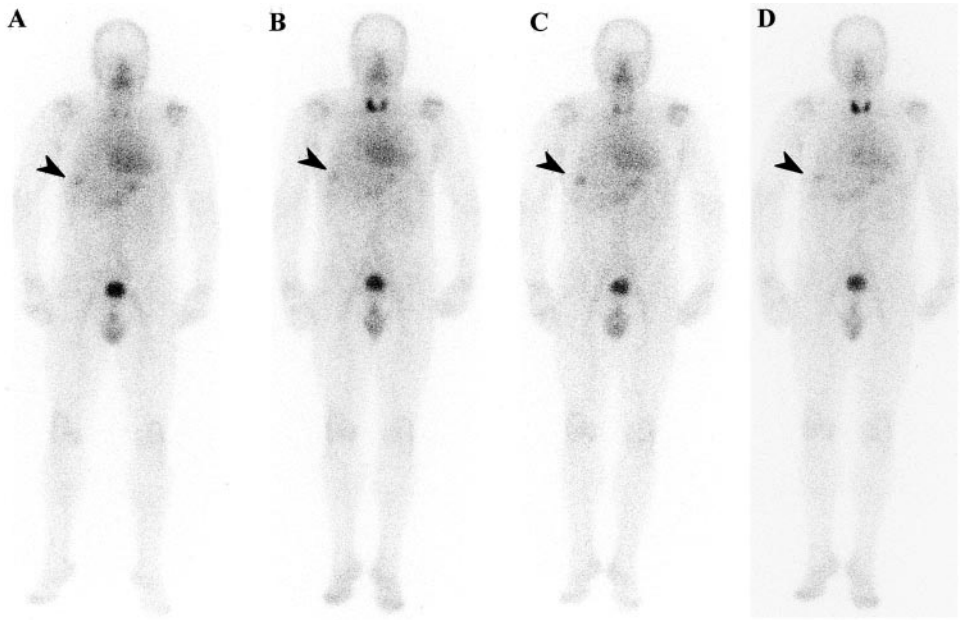

Fig. 3 Consistent targeting of [^{131}I]sibrotuzumab to metastatic colorectal carcinoma (*black arrow*) in patient 140 liver with repeat infusions over 2 cycles. Anterior whole body gamma camera images after infusion with 5 mg/m^2 [^{131}I]sibrotuzumab. *A*, day 5 1st infusion, cycle 1; *B*, day 5, 9th infusion, cycle 1; *C*, day 6, 1st infusion, cycle 2; *D*, day 6, 9th infusion, cycle 2.

Table 3 The relationship of HAHA to the biodistribution of [^{131}I]Sibrotuzumab, pharmacokinetics, and adverse events related to sibrotuzumab

Patient ID	Dose group (mg/m^2)	No. of infusions given	Infusion number at which HAHA first detectable		Peak HAHA level		Change in PK?	Change in biodistribution?	Related AE?
			ELISA	Biacore	ELISA (μg/ml)	Biacore (RU)[a]			
137	5	12	6	5	17.9	490	Y	Y	N
138	5	2	FU	FU	0.25	107	Y	ND	N
139	5	5	4	3	1.84	741	Y	Y	Y[b]
142	5	12	9	9	1.68	109	Y	Y	N
102	10	8	6	5	0.122	139	Y	Y	Y[c]
106	25	5	6	3	0.032	157	Y	Y	N
146	25	8	8	8	0.372	150	Y	ND	Y[b]
129	50	4	FU	4	0.53	113	Y	ND	Y[d]
				cutoff:	0.02	26			

[a] Abbreviations: RU, response units; ND, not determined—patients taken off study between positive HAHA result and next [^{131}I]sibrotuzumab infusion; Y, Yes; N, No; AE, adverse event; PK, pharmacokinetics; FU, 30 day follow-up sample after final infusion.
[b] CTC Grade 2.
[c] CTC Grade 1.
[d] CTC Grade 3 (back pain).

take, as well as reduced tumor uptake, and faster blood and whole body clearance of [^{131}I]sibrotuzumab. However, the total liver uptake and retention of [^{131}I]sibrotuzumab in these 3 patients was reduced compared with the first infusion. In the remaining 2 patients (patients 137 and 102), altered biodistribution was observed with faster whole body clearance and reduced tumor uptake, but no evidence of relative increased liver or spleen uptake. The presence of altered biodistribution corresponded with the development of faster serum pharmacokinetic measurements in patients compared with first infusion results.

Pharmacokinetics. A typical set of sibrotuzumab serum concentration-time curves measured by total ^{131}I radioactivity and ELISA is shown in Fig. 4. Overall, there was very good agreement between sibrotuzumab serum concentrations and pharmacokinetic parameters measured by the two methods. The mean terminal half-life ($t_{1/2\beta}$) of [^{131}I]sibrotuzumab based on serum radioactivity measurements increased with dose from 2.1 days (5 mg/m^2) to 5.2 days (50 mg/m^2), and the mean clearance decreased from 65 to 31 ml/h. C_{max} and AUC increased in a dose-dependent fashion (Table 4). There was no clear dose dependence of V_c (3.2–4.6 liters) or V_{ss} (4.2–5.9 liters). The data fitting yielded two-compartment kinetics, with 88–94% of AUC attributable to the elimination phase (Table 4). The mean terminal half-life of sibrotuzumab based on ELISA measurements increased with dose from 1.4 days (5 mg/m^2) to 4.9 days (50 mg/m^2), and the mean clearance decreased from 86 to 42 ml/h (Table 5). $C_{min(ss)}$, $C_{max(ss)}$, and AUC, which are measures

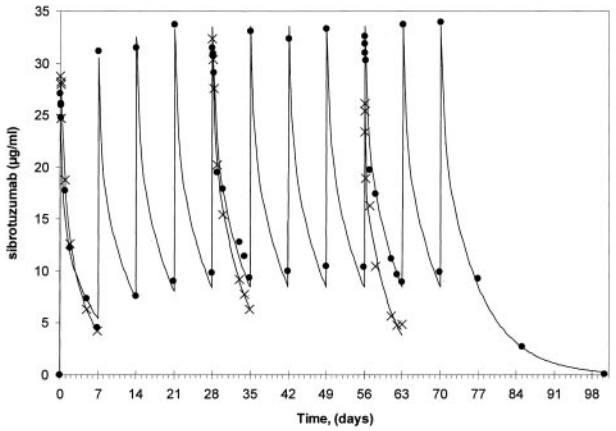

Fig. 4 Comparison of typical serum concentration-time profiles of sibrotuzumab measured as ^{131}I radioactivity (-×-) and by ELISA (-•-) for patient 145, 50 mg/m^2 dose level. The *symbols* indicate measured data, the *curves* represent 2-compartment model fits. No HAHA was evident in this patient.

of systemic exposure, increased dose-dependently. V_{ss} increased slightly from 3.9 to 5.5 liters over the dose range. The data fitting yielded one-compartment kinetics in the 5 and 10 mg/m^2 dose groups, and two-compartment kinetics in the 25 and 50 mg/m^2 dose groups. In the latter, >90% of AUC was attributable to the elimination phase.

HAHA. Of the 25 patients given ≥2 infusions of sibrotuzumab, HAHA responses occurred in 8 patients (32%) after 2–8 infusions. Only 4 of these patients experienced adverse events that were considered to be related to study drug (Table 3), and an additional 2 patients who experienced adverse events did not develop HAHA. The incidence of HAHA decreased with increasing dose, from 4 of 7 patients in the 5 mg/m^2 dose group to 1 of 6 patients at 50 mg/m^2.

The times of onset and the concentrations of HAHA attained were highly variable. The HAHA response increased with repeated dosing and persisted beyond the administration of the last infusion. The Biacore method appeared to be more sensitive than the ELISA regarding the detection of the first positive HAHA response (Table 3). Maximum HAHA levels (ELISA) ranged from 0.032 to 17.9 μg/ml (Table 3). The changes observed in the serum radioactivity profiles and the occurrence of interferences in sibrotuzumab serum concentration measurements by ELISA coincided with the time course of HAHA development. There was no correlation between the magnitude of HAHA levels and adverse events.

In Biacore blocking experiments sibrotuzumab blocked HAHA-positive sera completely, and mouse mAb F19 partially (data not shown). Human IgG1 control antibodies and mouse isotype control antibodies did not block HAHA-positive sera, indicating that the immune response was directed against epitopes located within the variable regions of sibrotuzumab.

Tumor Responses. At the end of the 12 weeks, 2 patients had stable disease and continued to receive unlabelled antibody. Patient 144 continued to receive sibrotuzumab at a dose of 50 mg/m^2 for 6 additional weekly infusions and then experienced disease progression. Patient 140 received a total of 108 weekly infusions of 5 mg/m^2 sibrotuzumab and then also experienced disease progression. Twenty-one patients had disease progression at the time of restaging. One patient was not assessed for tumor response.

DISCUSSION

This study is the first report of the successful targeting of a tumor stromal antigen in epithelial cancers in patients by a humanized mAb. Sibrotuzumab was well tolerated and could be safely administered by weekly infusion to patients with advanced FAP-positive malignancies. One episode of DLT was observed, and maximum tolerated dose was therefore not reached. Additional dose escalation was not performed in view of the lack of toxicity observed, the consistent biodistribution and tumor targeting demonstrated across dose levels, and the serum concentrations achieved. Of the 26 patients entered into the study, adverse events considered to be related to sibrotuzumab were observed in only 6 patients, and 3 of 6 patients were removed from study because of clinical immune responses associated with positive serum HAHA. Sibrotuzumab was administered for up to 108 infusions in 1 patient over a 2-year period, indicating the tolerance by patients of the treatment regime.

The biodistribution images of [^{131}I]sibrotuzumab showed minimal normal tissue uptake, with essentially blood pool distribution of [^{131}I]sibrotuzumab observed over a 1-week period. There was no difference in the biodistribution pattern of [^{131}I]sibrotuzumab between dose levels. Importantly, [^{131}I]sibrotuzumab showed rapid and selective uptake in sites of tumor, often by 1–2 days after infusion, and successfully targeted sites of disease in liver, lung, and soft tissue (Figs. 1–3). This finding of excellent tumor uptake at low protein doses in conjunction with the biodistribution data indicates that a large normal tissue antigen pool does not exist for FAP. This is distinct from other antibodies that target antigens that have high normal tissue expression (*e.g.*, rituximab, trastuzumab), where much higher protein doses are required to achieve comparable tumor uptake and serum concentrations. In the absence of HAHA, this biodistribution pattern and specific tumor uptake was observed in all of the patients for repeat [^{131}I]sibrotuzumab infusions during a 12-infusion treatment cycle. The biodistribution results are similar to that seen with prior studies with the murine form of sibrotuzumab (mAb F19), and provide additional evidence of the lack of normal tissue expression of the FAP antigen as a target for sibrotuzumab.

Sibrotuzumab exhibited moderately nonlinear one- or two-compartment pharmacokinetics in this study population; the terminal phase $t_{1/2}$ (based on ELISA) ranged from 1.4 to 4.9 days over the dose range 5–50 mg/m^2. The good agreement between serum concentrations and pharmacokinetic parameters determined by radioactivity and the ELISA method indicates that the ^{131}I radioisotope label is metabolically stable *in vivo*.

The half-life of sibrotuzumab found in this study is rather short compared with available literature data on the pharmacokinetics of humanized antibodies, in which half-lives in the range of 6–20 days have been reported (21–23) at various antibody doses. It is possible that the murine complementarity determining region and residual framework segments of sibro-

Table 4 Mean pharmacokinetic parameters of [^{131}I]Sibrotuzumab based on total radioactivity

Dose group (mg/m^2)	n^a		C_{max} (μg/ml)	CL (ml/h)	V_c (liter)	V_{ss} (liter)	$t_{1/2\alpha}$ (h)	$t_{1/2\beta}$ (day)	AUC (μg*h/ml)	AUC_β (%)
5	16	Mean	2.67	64.5	3.43	4.17	6.88	2.12	154	94.0
		SD	0.336	17.2	0.633	0.744	7.51	0.81	35.5	9.40
10	11	Mean	5.47	62.9	3.63	4.18	8.70	2.25	345	93.3
		SD	0.865	27.3	0.940	0.887	8.74	0.85	109	9.39
25	6	Mean	12.12	64.5	4.60	5.85	13.74	2.94	883	87.7
		SD	1.50	6.64	0.66	0.88	10.51	0.70	136	12.78
50	12	Mean	29.5	30.9	3.15	4.64	13.0	5.21	3300	92.6
		SD	3.03	9.97	0.318	0.803	10.2	2.40	881	6.90

[a] *n* indicates the number of single dose data sets used that were not affected by HAHA development. Includes data after infusions 1, 5, and 9 for each subject when available, and data from the additional treatment cycles of patient 140 in the 5 mg/m^2 dose group.

Table 5 Mean pharmacokinetic parameters of sibrotuzumab measured by ELISA

Dose group (mg/m^2)	*n*		$C_{min_{(ss)}}$ (μg/ml)	$C_{max_{(ss)}}$ (μg/ml)	CL (ml/h)	V_c[a] (liter)	V_{ss} (liter)	$t_{1/2\alpha}$[a] (h)	$t_{1/2\beta}$ (day)	AUC (μg*h/ml)	AUC_β (%)
5	7	Mean	0.0779	2.53	86.3	—	3.90	—	1.36	105	—
		SD	0.061	0.38	21.7	—	0.78	—	0.29	34.9	—
10	6	Mean	0.343	5.07	87.8	—	4.83	—	1.76	275	—
		SD	0.272	1.41	53.9	—	1.97	—	0.41	119	—
25	6	Mean	1.61	12.8	65.4	4.52	5.46	10.1	2.62	929	94.4
		SD	0.60	1.2	15	1.13	1.40	12.1	0.82	85.3	11.4
50	7	Mean	7.73	31.0	41.9	3.85	5.47	16.6	4.86	2610	90.4
		SD	5.14	5.6	16	0.419	1.36	10.1	2.52	971	11.2

[a] Not available for subjects who exhibited one-compartment kinetics.

tuzumab contribute significantly to the pharmacokinetics of this humanized IgG1. Other pharmacokinetic parameters are similar to known data for physiological IgG. The initial volume of distribution (V_c) of 3.9–4.5 liters corresponds approximately to the serum volume, and V_{ss} was only slightly higher (up to 5.5 liters) indicating limited distribution of sibrotuzumab outside the blood compartment. The trend toward a decrease of clearance and increase of terminal half-life of sibrotuzumab with increasing dose may be attributable to saturation of a clearance mechanism of the antibody. The biological rationale for this kinetic nonlinearity is not known. The lack of normal tissue uptake of sibrotuzumab on biodistribution images would indicate that FAP expression in normal tissues would be highly unlikely to explain the pharmacokinetic results observed. The relatively short half-life of sibrotuzumab could be advantageous for radioimmunotherapy because it would limit bone marrow exposure, which is the expected DLT for radioisotope-labeled sibrotuzumab.

The incidence of HAHA was 8 of 25 patients (32%), and occurred after 2–8 weekly infusions of sibrotuzumab. Whereas HAHA incidence appeared to decrease at higher doses, this may merely reflect the small numbers of patients included in each dose cohort. The occurrence of HAHA as measured by double-antigen ELISA and Biacore coincided with an increase in clearance and volume of distribution measured by [^{131}I]sibrotuzumab serum radioactivity, but did not correlate with the magnitude of related adverse events, with only 4 of 8 patients with positive HAHA demonstrating symptoms attributable to HAHA. The development of HAHA was also associated with altered biodistribution, compared with first infusion image datasets, in all 5 of the patients with HAHA present at the time of an [^{131}I]sibrotuzumab infusion. This change in biodistribution did not result in an increase in uptake and retention of [^{131}I]sibrotuzumab in the whole body or normal organs dosimetry analysis, compared with the first infusion, in any of these patients (data not shown). Importantly, when HAHA was negative at the time of [^{131}I]sibrotuzumab infusion, all of the patients had unaltered biodistribution. This direct correlation between HAHA measurements and biodistribution patterns indicates that HAHA measurements are predictive of altered biodistribution, and could be used to indicate suitability for repeat doses of radiolabelled sibrotuzumab in future trials.

The ability to target FAP in the stroma of tumors with repeat infusions of sibrotuzumab demonstrated in this trial provides evidence that sibrotuzumab has promise in the targeting and therapy of epithelial malignancies. Although 1 patient had stable disease for 2 years while receiving sibrotuzumab infusions, this study did not address the efficacy of sibrotuzumab, and additional Phase I/II trials of sibrotuzumab in patients with FAP-positive malignancies, assessing the safety and efficacy of unlabelled and radiolabelled sibrotuzumab, have been initiated.

REFERENCES

1. Dvorak, H. F. Tumors: wounds that do not heal. Similarities between tumor stroma generation and wound healing. N. Engl. J. Med., *315:* 1650–1659, 1986.

2. Iozzo, R. V. Tumor stroma as a regulator of neoplastic behavior. Agonistic and antagonistic elements embedded in the same connective tissue. Lab. Investig., *73:* 157–160, 1995.

3. Garin-Chesa, P., Old, L. J., and Rettig, W. J. Cell surface glycoprotein of reactive stromal fibroblasts as a potential antibody target in human epithelial cancers. Proc. Natl. Acad. Sci. USA, *87:* 7235–7239, 1990.

4. Van den Eynde, B. J., and Scott, A. M. Tumor antigens. *In:* P. J. Delves and I. M. Roitt (eds.), Encylopedia of Immunology, Ed. 2, Vol. 4, pp. 2424–2431. London: Academic Press, 1998.

5. Rettig, W. J., Garin-Chesa, P., Beresford, H. R., Oettgen, H. F., Melamed, M. R., and Old, L. J. Cell-surface glycoproteins of human sarcomas: differential expression in normal and malignant tissues and cultured cells. Proc. Natl. Acad. Sci. USA, *85:* 3110–3114, 1988.

6. Levy, M. T., McCaughan, G. W., Abbott, C. A., Park, J. E., Cunningham, A. M., Muller, E., Rettig, W. J., and Gorrell, M. D. Fibroblast activation protein: a cell surface dipeptidyl peptidase and gelatinase expressed by stellate cells at the tissue remodelling interface in human cirrhosis. Hepatology, *29:* 1768–1778, 1999.

7. Rettig, W. J., Su, S. L., Fortunato, S. R., Scanlan, M. J., Raj, B. K., Garin-Chesa, P., Healey, J. H., and Old, L. J. Fibroblast activation protein: purification, epitope mapping and induction by growth factors. Int. J. Cancer, *58:* 385–392, 1994.

8. Rettig, W. J., Garin-Chesa, P., Healey, J. H., Su, S. L., Ozer, H. L., Schwab, M., Albino, A. P., and Old, L. J. Regulation and heteromeric structure of the fibroblast activation protein in normal and transformed cells of mesenchymal and neuroectodermal origin. Cancer Res., *53:* 3327–3335, 1993.

9. Scanlan, M. J., Raj, B. K., Calvo, B., Garin-Chesa, P., Sanz-Moncasi, M. P., Healey, J. H., Old, L. J., and Rettig, W. J. Molecular cloning of fibroblast activation protein α, a member of the serine protease family selectively expressed in stromal fibroblasts of epithelial cancers. Proc. Natl. Acad. Sci. USA, *91:* 5657–5661, 1994.

10. Mathew, S., Scanlan, M. J., Mohan Raj, B. K., Murty, V. V., Garin-Chesa, P., Old, L. J., Rettig, W. J., and Chaganti, R. S. The gene for fibroblast activation protein α (FAP), a putative cell surface-bound serine protease expressed in cancer stroma and wound healing, maps to chromosome band 2q23. Genomics, *25:* 335–337, 1995.

11. Niedermeyer, J., Scanlan, M. J., Garin-Chesa, P., Daiber, C., Fiebig, H. H., Old, L. J., Rettig, W. J., and Schnapp, A. Mouse fibroblast activation protein: molecular cloning, alternative splicing and expression in the reactive stroma of epithelial cancers. Int. J. Cancer, *71:* 383–389, 1997.

12. Park, J. E., Lenter, M. C., Zimmermann, R. N., Garin-Chesa, P., Old, L. J., and Rettig, W. J. Fibroblast activation protein, a dual specificity serine protease expressed in reactive human tumor stromal fibroblasts. J. Biol. Chem., *274:* 36505–12, 1999.

13. Cheng, J. D., Dunbrack, R. L., Jr., Valianou, M., Rogatko, A., Alpaugh, R. K., and Weiner, L. M. Promotion of tumor growth by murine fibroblast activation protein, a serine protease, in an animal model. Cancer Res., *62:* 4767–4772, 2002.

14. Welt, S., Divgi, C. R., Scott, A. M., Garin-Chesa, P., Finn, R. D., Graham, M., Carswell, E. A., Cohen, A., Larson, S. M., Old, L. J., and *et al.* Antibody targeting in metastatic colon cancer: a phase I study of monoclonal antibody F19 against a cell-surface protein of reactive tumor stromal fibroblasts. J. Clin. Oncol., *12:* 1193–203, 1994.

15. Tanswell, P., Garin-Chesa, P., Rettig, W. J., Welt, S., Divgi, C. R., Casper, E. S., Finn, R. D., Larson, S. M., Old, L. J., and Scott, A. M. Population pharmacokinetics of antifibroblast activation protein monoclonal antibody F19 in cancer patients. Br. J. Clin. Pharmacol., *51:* 177–180, 2001.

16. Riechmann, L., Clark, M., Waldmann, H., and Winter, G. Reshaping human antibodies for therapy. Nature (Lond.), *332:* 323–327, 1988.

17. Lee, F. T., Hall, C., Rigopoulos, A., Zweit, J., Pathmaraj, K., O'Keefe, G. J., Smyth, F. E., Welt, S., Old, L. J., and Scott, A. M. Immuno-PET of human colon xenograft- bearing BALB/c nude mice using 124I-CDR-grafted humanized A33 monoclonal antibody. J. Nucl. Med., *42:* 764–769, 2001.

18. Heinzel, G., Woloszczak, W., and Thomann, P. TopFit: Pharmacokinetic and Pharmacodynamic Data Analysis System for the PC., Version 2.0 edition. Stuttgart: Gustav Fischer Verlag, 1993.

19. Ritter, G., Cohen, L. S., Williams, C., Jr., Richards, E. C., Old, L. J., and Welt, S. Serological analysis of human anti-human antibody responses in colon cancer patients treated with repeated doses of humanized monoclonal antibody A33. Cancer Res., *61:* 6851–6859, 2001.

20. LoBuglio, A. F., Wheeler, R. H., Trang, J., Haynes, A., Rogers, K., Harvey, E. B., Sun, L., Ghrayeb, J., and Khazaeli, M. B. Mouse/human chimeric monoclonal antibody in man: kinetics and immune response. Proc. Natl. Acad. Sci. USA, *86:* 4220–4224, 1989.

21. Wiseman, L. R., and Faulds, D. Daclizumab: a review of its use in the prevention of acute rejection in renal transplant recipients. Drugs, *58:* 1029–1042, 1999.

22. Baselga, J., Tripathy, D., Mendelsohn, J., Baughman, S., Benz, C. C., Dantis, L., Sklarin, N. T., Seidman, A. D., Hudis, C. A., Moore, J., Rosen, P. P., Twaddell, T., Henderson, I. C., and Norton, L. Phase II study of weekly intravenous recombinant humanized anti-p185HER2 monoclonal antibody in patients with HER2/neu-overexpressing metastatic breast cancer. J. Clin. Oncol., *14:* 737–744, 1996.

23. Everitt, D. E., Davis, C. B., Thompson, K., DiCicco, R., Ilson, B., Demuth, S. G., Herzyk, D. J., and Jorkasky, D. K. The pharmacokinetics, antigenicity, and fusion-inhibition activity of RSHZ19, a humanized monoclonal antibody to respiratory syncytial virus, in healthy volunteers. J. Infect. Dis., *174:* 463–469, 1996.

Clinical Cancer Research

A Phase I Dose-Escalation Study of Sibrotuzumab in Patients with Advanced or Metastatic Fibroblast Activation Protein-positive Cancer

Andrew M. Scott, Greg Wiseman, Sydney Welt, et al.

Clin Cancer Res 2003;9:1639-1647.